Hindawi
Wireless Communications and Mobile Computing
Volume 2019, Article ID 5864657, 16 pages
https://doi.org/10.1155/2019/5864657

Research Article

Cross-Layer Resource Allocation for Multihop V2X Communications

Yanhua He,[1] **Liangrui Tang**,[1] **Yun Ren**,[2] **Jonathan Rodriguez**,[3] **and Shahid Mumtaz**[4]

[1]*The State Key Laboratory of Alternate Electrical Power System with Renewable Energy Sources, School of Electrical and Electronic Engineering, North China Electric Power University, Beijing 102206, China*
[2]*State Grid Zhejiang Electric Power Company Ningbo Bureau, Zhejiang 315000, China*
[3]*University of South Wales, Pontypridd, CF37 1DL, UK*
[4]*Instituto de Telecomunicações, Distrito de Aveiro 3810-193, Portugal*

Correspondence should be addressed to Yanhua He; yanhuahe91927@163.com

Received 16 November 2018; Accepted 22 January 2019; Published 12 February 2019

Academic Editor: Mohammed El-Hajjar

Inspired by the increasingly mature vehicle-to-everything (V2X) communication technology, we propose a multihop V2X downlink transmission system to improve users' quality of experience (QoE) in hot spots. Specifically, we develop a cross-layer resource allocation algorithm to optimize the long-term system performance while guaranteeing the stability of data queues. Lyapunov optimization is employed to transform the long-term optimization problem into a series of instantaneous subproblems, which involves the joint optimization of rate control, power allocation, and mobile relay selection at each time slot. On one hand, the optimization of rate control is decoupled and carried out independently. On the other hand, a low-complexity pricing-based stable matching algorithm is proposed to solve the joint power allocation and mobile relay selection problem. Finally, simulation results demonstrate that the proposed algorithm can achieve superior performance and simultaneously guarantee queue stability.

1. Introduction

With the explosive growth of mobile Internet and the rapid expansion of massive data traffic services, mobile communication systems put forward higher requirements for network capacity, especially in hot spots with high user density. In this case, users' quality of experience (QoE) will drop sharply due to the limited network resources and the possibility of blocking and packet loss. Consequently, the reliability of wireless communication system cannot be guaranteed [1, 2].

To address this challenge, many researchers have proposed deploying more microcells, picocells, or relays, expecting to increase the capacity and coverage of the network [3]. However, these methods introduce new problems, such as large energy consumption, high deployment and maintenance cost, and so on [4–6]. Therefore, wireless communication systems urgently thirst for a solution which has flexible application range, low deployment cost, and simple network maintenance.

On the other hand, the development of vehicular networks becomes more and more mature [7, 8]. Vehicle to everything (V2X), which includes vehicle-to-vehicle (V2V), vehicle-to-pedestrian (V2P), vehicle-to-infrastructure (V2I), and vehicle-to-network (V2N) communications, plays an important role in improving road safety, traffic efficiency, and service reliability [9]. Moreover, the integration of vehicular networks and cellular networks, i.e., cellular V2X (C-V2X), provides better performance guarantee under high load conditions. In other words, V2X technology also makes it possible to use vehicles as mobile relays to augment network connectivity, expand network capacity, and improve users' QoE and quality of service (QoS) [10–12].

However, establishing this V2X-based multihop relay system faces the following major challenges. First, how to control the stability of data queues considering the dynamic data arrival and departure remains an open issue. It involves not only the optimization of rate control at the network layer but also the optimization of power allocation and relay

selection in the physical layer. Therefore, the traditional resource allocation of physical layer scheme will no longer be applicable, and a cross-layer resource optimization scheme is needed. Second, the joint optimization of rate control, power allocation, and relay selection is formulated as a mixed integer nonlinear optimization problem, since both binary and continuous optimization variables are involved. How to solve this nonlinear optimization problem effectively is another challenge. Last but not least, conventional resource allocation schemes mainly focus on short-term optimization and ignore long-term system performance and constraints. At each round of optimization, the resources are allocated in a greedy way without considering the future, which results in long-term performance degradation. However, it is infeasible to derive the optimal long-term optimization solution due to the absence of the future knowledge. Therefore, how to achieve low-complexity online resource allocation with guaranteed performance requires further study.

To tackle these challenges, we propose a multihop V2X communication system to improve the network capacity and realize the long-term reliable transmission for users densely distributed in hot spots. It mainly involves the rate control in the network layer, as well as the mobile relay selection and power allocation in the physical layer. The objective is to optimize the long-term users' QoE performance under the constraints of long-term power consumption and queue stability.

The main contributions of this paper are summarized as follows:

(i) A multihop downlink communication system based on V2X is established. In this system, vehicles as mobile relays play the roles of transmitting traffic from BS to users. In such system, vehicles are not only extensions of base station (BS) transmission distance, but also methods for BS to expand coverage and improve system throughput.

(ii) A cross-layer long-term optimization is established for the multihop V2X communication system. Such long-term optimization cannot be resolved by existing approaches. Motivated by this, the recently-developed Lyapunov optimization approach is leveraged. With its assistance, the long-term optimization problem is transformed into a gradual optimization problem. First, the long-term optimization is formulated to obtain the optimal long-term QoE under the constraints of long-term power consumption and delay. Second, the constraints of long-term power consumption and delay are transformed into virtual queues stability problem. Finally, the long-term performance optimization is decomposed into a series of online subproblems involving trading off queue backlog and utility.

(iii) An online algorithm based on Lyapunov optimization is proposed. The above mentioned online subproblem is divided into the rate control problem in network layer and the resource allocation problem in physical layer. Faced with this, the rate control problem is solved by the convex optimization easily. However, the physical layer resource allocation problem, as a mixed integer nonlinear optimization problem, is difficult to be solved. Further, we prove that the resource allocation problem is a convex problem, given the mobile relay selection results. In the sense, the price-based matching is proposed to deal with the mobile relay selection problem. This online algorithm only needs to know the current channel and queue information, without foreknowledge of global information. These works successfully reduce the signalling overheads and computational complexity and conform to the time causality.

The rest of this paper is organized as follows. The related work is introduced in Section 2. The system model and problem formulation are described in Sections 3 and 4. In Section 5, Lyapunov optimization approach is applied to converting the original long-term optimization problem into a series of rate control and power allocation problems to be optimized in each timeslot, and the matching is introduced to solve the mobile relay selection problem. Simulation results and the associated discussions are presented in Section 6, and the conclusions of this paper are drawn in Section 7.

2. Related Work

The concept of V2X communication which helps to support variety of traffic-efficient applications has drawn great attention in both industrial and academic fields recently [10, 13, 14]. In [10], Ashraf et al. developed a novel QoS-aware resource allocation scheme for V2V communication. A joint resource block (RB) allocation and power control algorithm was proposed in [13] for radio resource management of device-to-device (D2D) based V2V communications. The authors in [14] proposed an energy sensing-based spectrum sharing mechanism which can reduce the transmission collisions between cellular V2X and vehicular ad hoc network (VANET) users by allowing cellular V2X users to use unlicensed channels fairly. These works mainly regard vehicles as terminal users but have not taken into account the network capacity expansion by adopting vehicles as mobile relays.

Several works have focused on the service queue stability to improve users' QoE [15–18]. In [15], a cluster-based heterogeneous vehicular networks (C-HetVNETs) framework with dynamic data arrival was developed, and the performance metrics including delay, throughput, and queue length are analyzed based on a Markov queuing model. Two queue-aware power allocation schemes in V2V networks were proposed in [16], which characterized the statistics of extreme events according to the maximal queue length by extreme value theory. The authors in [17] presented a joint power allocation and subcarrier scheme in the downlink of an OFDMA system, in which the rate constraints were defined in order to guarantee queue stability. In [18], queue theory was used to analyze the performance of arrival and the service curve to guarantee queue stability, and the proposed traffic flow model was verified by a M/M/c model. The control of queue stability in these works generally assumed that the complete state information is known, while it is optimistic

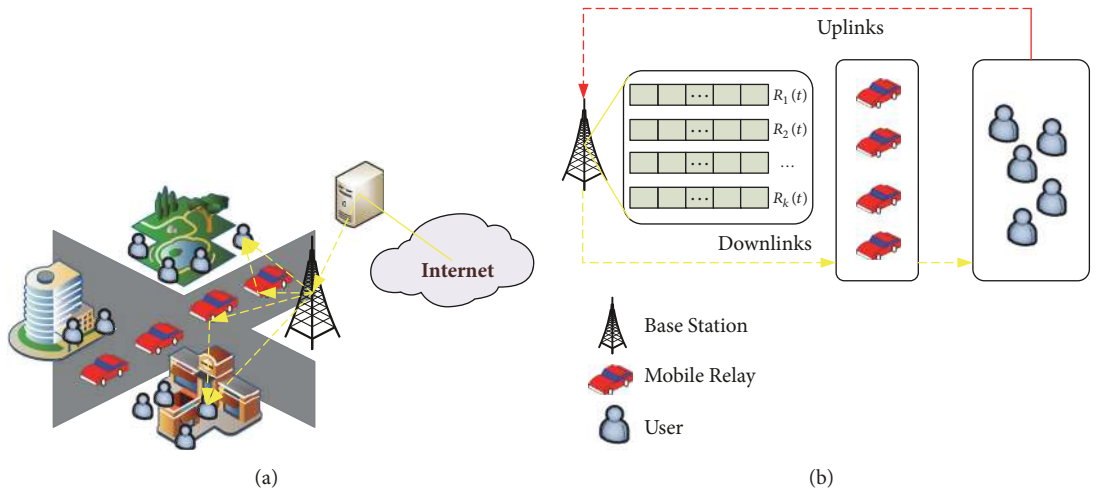

FIGURE 1: System model. (a) V2X communications system. (b) Queue diagram of the system.

to get perfect information in advance. On the other hand, the traditional methods of processing queues own a higher computational complexity in practical implementations.

Resource allocation problems in V2X communication have been studied in [19–22]. A joint optimization of the radio resource and power allocation algorithm was proposed in [19] to maximize the service rate of cellular user equipment (UE). In [20, 21], a two-stage resource allocation algorithm based on auction matching and nonlinear fractional programming was presented in vehicular heterogeneous networks. An uplink radio resource allocation scheme for V2V communication in freeway scenario was proposed in [22], which aimed to maximize the sum rate of V2V links, while the transmission requirements of vehicular UEs were neglected. These resource allocation schemes for V2X communications mainly focus on short-term designs, i.e., implementing optimization in a single time slot while ignoring the practical long-term constraints.

3. System Model

Figure 1(a) shows the proposed V2X communication systems. We consider a downlink data transmission in a dense network with one BS and K users. Moreover, we assume the users are heterogeneous, so that users' traffic could be classified as K types. There also are N vehicles. For users, these vehicles play the roles of mobile relays using the amplify and forward (AF) protocol. To proceed, assume these vehicles running at a constant speed and in the same direction. Further, the users' set is presented by $\mathbf{K} = \{1, 2, \cdots k, \cdots, K\}$, and the vehicles' set is presented by $\mathbf{N} = \{1, 2, \cdots, n, \cdots, N\}$.

The system operates in a time-slotted manner with timeslot index $t \in \{0, 1, 2, \cdots\}$. At timeslot t, $R_k(t)$ bits traffic data arrive at BS for user k. So define the $Q_k(t)$ as the amount of data buffered at queue k for user k at timeslot t. The queue model is shown in the Figure 1(b). In this system, the buffer size is enough and packet loss incidents will not happen. To proceed, let $C_k(t)$ denote the amount of traffic data that could be delivered to user k. In fact, $C_k(t)$ could be seen as transmission capacity of the V2X system for the k-th user. Then, the dynamics queue corresponding to the k-th queue can be characterized as

$$Q_k(t+1) = \max\left[Q_k(t) - C_k(t), 0\right] + R_k(t) \tag{1}$$

It is worth noting that $R_k(t)$ and $C_k(t)$ are indicators that belong to different layers. $R_k(t)$ is the traffic from Internet, buffered at BS and transmitted to user k. Correspondingly, one of the network layer functions is to control the traffic from the source node to the destination node. So $R_k(t)$ corresponds to network layer. In addition, $C_k(t)$ completes the functions of the physical layer, implementing transparent transmission of the bit stream.

As we know, the higher data rate brings more enjoyable experience to users. However, marginal utility theory sets forth a viewpoint: When other inputs remain unchanged, increasing a certain input continuously will result in a gradual decrease in the new income. On this basis, we define QoE $U_k(t)$ to describe the satisfaction of user k, which is shown as [23]

$$U_k(t) = \chi_k \log_2\left[1 + R_k(t)\right] \tag{2}$$

χ_k represents the degree of preference of BS to the k-th type service. The larger χ_k is, the more data user k will receive. The logarithmic function describes that the marginal increment of QoE declines gradually with $R_k(t)$, but the QoE is increasing continuously.

To improve the transmission capacity of the downlink, AF protocol is applied to vehicles with single antenna, which are called mobile relays in this paper.

As illustrated in Figure 2, the AF collaboration system is composed of a single source node, i.e., BS, single relay node, i.e., the n-th mobile relay, and a single destination node, i.e., the k-th user. The mobile relay just acts as a helper for BS and does not have any own information to send. In this paper, the frequency band of BS is orthogonally assigned to the K queues.

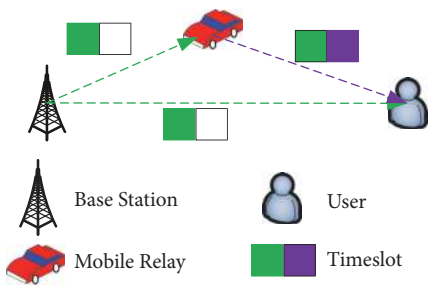

Figure 2: AF collaboration system model.

The mobile relay is assumed to be operated in half-duplex mode; i.e., it cannot transmit and receive simultaneously. The transmission from BS and the relay node are done over orthogonal channels in time domain [24]. In the first half of the timeslot, BS broadcasts its signal to the destination and the mobile relay. The received signal-to-noise ratios (SNR) are

$$SNR_k^{AF}(\mathrm{t}) = \sum_{n=1}^{N} w_{k,n}(t)\frac{P_k(t)}{N_0}\left|h_{k,n}(t)\right|^2 \tag{3}$$

$$SNR_{k,u}^{DL}(t) = \frac{P_k(t)}{N_0}\left|h_{k,u}(t)\right|^2 \tag{4}$$

Then, according to AF protocol, the mobile relay node forwards the source signal to user over the remaining time. The received SNR after amplifying is expressed as follows:

$$SNR_u^{AF}(t) = \sum_{n=1}^{N} w_{k,n}(t)\frac{P_n(t)}{N_0}\left|h_{n,u}(t)\right|^2 \tag{5}$$

Here, $SNR_k^{AF}(\mathrm{t})$ is the received SNR of mobile relay for user k. $SNR_{k,u}^{DL}(t)$ is the received SNR of user k by the direct link from BS. $SNR_u^{AF}(t)$ is the received SNR of user k from the amplified signal by mobile relay.

N_0 is the Gaussian white noise, $P_k(t)$ is the transmit power allocated by BS to transfer data of queue k belonged to user k at the timeslot t, and $P_n(t)$ is the transmit power of mobile relay n. $h_{k,n}(t)$, $h_{k,u}(t)$, and $h_{n,u}(t)$ are the fading coefficients of BS to mobile relay n, BS to users and mobile relay n to users on Rayleigh channel links obeying the complex Gaussian distribution. $h_{k,n}(t)$, $h_{k,u}(t)$, and $h_{n,u}(t)$ are i.i.d. over time and remain unchanged at each timeslot but change from slot to slot. $w_{k,n}(t) \in \{0,1\}$, if queue k accesses the mobile relay n, $w_{k,n}(t) = 1$; otherwise, $w_{k,n}(t) = 0$.

When users receive signals with maximum ratio combining (MRC) [25, 26], the available maximum average transmission capacity for the k-th user is

$$C_k(t) = \frac{F}{2} \cdot \log_2\left\{1 + SNR_{k,u}^{DL}(t) + f\left[SNR_k^{AF}(\mathrm{t}), SNR_u^{AF}(t)\right]\right\} \tag{6}$$

where $f(x,y) = xy/(1+x+y)$ and F is the bandwidth allocated to queue k.

To be simple, this paper just considers the power allocation of BS to the queues, and the transmission power of relay is fixed. The queues' transmission power is constrained by two practical limitations. One is inspired with the energy saving of BS, which is to limit the long-term averaged power consumption and it is set as

$$0 \le \lim_{T\to\infty}\frac{1}{T}\sum_{t=1}^{T}\mathbb{E}\left[\sum_{k=1}^{K}\sum_{n=1}^{N} w_{k,n}(t)P_{k,n}(t)\right] \le P_{ave} \tag{7}$$

P_{ave} is the long-term maximum average power consumption. The other one is a regular instantaneous limit, which is set as

$$0 \le \sum_{n=1}^{N} w_{k,n}(t)P_{k,n}(t) \le P_{\max} \quad \forall k,t \tag{8}$$

4. Problem Formulation

The aim of this paper is to maximize the long-term QoE of this system, which is shown as

$$\begin{aligned}
\max_{\mathbf{R(t)},\mathbf{P(t)},\mathbf{w(t)}} \quad & \lim_{T\to\infty}\frac{1}{T}\sum_{t=1}^{T}\sum_{k=1}^{K}U_k(t) \\
s.t. \quad & C1: \lim_{T\to\infty}\frac{\mathbb{E}\left[Q_k(t)\right]}{T} = 0 \quad \forall k \\
& C2: 0 \le \sum_{n=1}^{N} w_{k,n}(t)P_{k,n}(t) \le P_{\max} \quad \forall k,t \\
& C3: \lim_{T\to\infty}\frac{1}{T}\sum_{t=1}^{T}\mathbb{E}\left[\sum_{k=1}^{K}\sum_{n=1}^{N} w_{k,n}(t)P_{k,n}(t)\right] \\
& \le P_{ave} \\
& C4: \theta_k(t) \le D_k(t) \quad \forall k,t \\
& C5: w_{k,n}(t) \in \{0,1\} \quad \forall k,n,t \\
& C6: \sum_{n=1}^{N} w_{k,n}(t) = 1 \quad \forall k,t \\
& C7: \sum_{k=1}^{K} w_{k,n}(t) = 1 \quad \forall n,t \\
& C8: 0 \le \sum_{k=1}^{K} R_k(t) \le R_{\max} \quad \forall k,t
\end{aligned} \tag{9}$$

where $\mathbf{R(t)} = [R_1(t), R_2(t), \cdots R_K(t)]$, $\mathbf{P(t)} = [P_1(t), P_2(t), \cdots P_K(t)]$, and $\mathbf{w(t)}$ is the mobile relay selection matrix. The constraint $C1$ guarantees that $Q_k(t)$ is mean rate stable, which indicates the queue will be stable at a finite value finally. $C2$ and $C3$ are the constraints of power. $\theta_k(t)$ is the queuing delay defined as the time that a packet waits in a queue until it can be transmitted to the users. Moreover, $D_k(t)$ defines the upper bound of the queuing delay. $C6$ and $C7$ suggest that each queue only accesses one relay and each relay only services one

queue. $C8$ constrains the data amount of queue k admitted within the system at timeslot t.

Due to the queuing model (1) and the long-term average power constraint (6), rate control (RC) and mobile relay selection and power allocation (RSPA) are tangled together across layers. In the sense, (9) is difficult to be solved. To address the challenges, Lyapunov optimization technique is developed [27, 28]. Lyapunov optimization technique deals with such problems without prior information and has low computational complexity.

5. Online Algorithm Based on Lyapunov Optimization

Lyapunov optimization is efficient in designing stable control algorithms. It has been extended to treat network stability and performance optimization simultaneously. In this section, the online algorithm based on Lyapunov optimization toward (9) is evolved.

5.1. Lyapunov Optimization. The long-term power constraint $C3$ could be transferred to a virtual queue stability problem. The power-constrained virtual queue is formulated as $E(t)$ with $E(0) = 0$, and the update equation is

$$E(t+1) = \max\left[E(t) - P_{ave}, 0\right] + Y(t) \tag{10}$$

where $Y(t) = \sum_{k=1}^{K}\sum_{n=1}^{N} w_{k,n}(t)P_{k,n}(t)$ is the power consumption of BS at timeslot t. If $E(t)$ tends to mean rate stable, the long-term average power constraint will be satisfied [29].

Similarly, the delay-constrained virtual queue $Z_k(t)$ is defined as

$$Z_k(t+1) = \max\left[Z_k(t) - C_k(t)D_k(t), 0\right] + Q_k(t) \tag{11}$$

Physically speaking, (11) indicates that if traffic of queue k cannot all be transmitted within the upper bound of the delay, and then the rest of the traffic will be backlogged to be transmitted in the next time slot.

Subsequently, let $\mathbf{G(t)} = [\mathbf{Q(t)}, E(t), \mathbf{Z(t)}]$ be a concatenated vector, where $\mathbf{Q(t)} = [Q_1(t), Q_2(t), \cdots, Q_k(t)]$ and $\mathbf{Z(t)} = [Z_1(t), Z_2(t), \cdots, Z_k(t)]$. The Lyapunov function is $L[\mathbf{G(t)}]$:

$$L[\mathbf{G}(\mathbf{t})] = \frac{1}{2}\sum_{k=1}^{K} Q_k^2(t) + \frac{1}{2}E^2(t) + \frac{1}{2}\sum_{k=1}^{K} Z_k^2(t) \tag{12}$$

Then the Lyapunov drift is denoted as

$$\Delta[\mathbf{G}(\mathbf{t})] = \mathbb{E}\left\{L[\mathbf{G}(\mathbf{t+1})] - L[\mathbf{G}(\mathbf{t})] \mid \mathbf{G}(\mathbf{t})\right\} \tag{13}$$

We can obtain the drift minus utility function as

$$\Delta[\mathbf{G}(\mathbf{t})] - V\mathbb{E}\left\{\sum_{k=1}^{K} U_k(t) \mid \mathbf{G}(\mathbf{t})\right\} \tag{14}$$

where V is a tuneable weight, which controls the tradeoff between the drift $\Delta[\mathbf{G(t)}]$ and the utility $\mathbb{E}[\sum_{k=1}^{K} U_k(t) \mid \mathbf{G(t)}]$.

The drift minus utility function is further bounded in the following way:

$$\begin{aligned}
&\Delta[\mathbf{G}(\mathbf{t})] - V\mathbb{E}\left[\sum_{k=1}^{K} U_k(t) \mid \mathbf{G}(\mathbf{t})\right] \\
&\le \frac{1}{2}\sum_{k=1}^{K}\mathbb{E}\left[C_k^2(t)\right] + \frac{1}{2}\sum_{k=1}^{K}\mathbb{E}\left[R_k^2(t)\right] \\
&\quad + \sum_{k=1}^{K} Q_k(t)\,\mathbb{E}\left[R_k(t) - C_k(t) \mid \mathbf{G}(\mathbf{t})\right] \\
&\quad + \frac{1}{2}\mathbb{E}\left[P_{ave}^2(t)\right] + \frac{1}{2}\mathbb{E}\left[Y^2(t)\right] \\
&\quad + E(t)\,\mathbb{E}\left[Y(t) - P_{ave} \mid \mathbf{G}(\mathbf{t})\right] + \frac{1}{2}\sum_{k=1}^{K}\mathbb{E}\left[Q_k^2(t)\right] \\
&\quad + \frac{1}{2}\sum_{k=1}^{K}\mathbb{E}\left[C_k^2(t)D_k^2(t)\right] \\
&\quad + \sum_{k=1}^{K} Z_k(t)\,\mathbb{E}\left[Q_k(t) - C_k(t)D_k(t) \mid \mathbf{G}(\mathbf{t})\right] \\
&\quad - V\mathbb{E}\left[\sum_{k=1}^{K} U_k(t) \mid \mathbf{G}(\mathbf{t})\right]
\end{aligned} \tag{15}$$

Let

$$\begin{aligned}
&B \ge B(t) \\
&= \frac{1}{2}\sum_{k=1}^{K}\mathbb{E}\left[C_k^2(t)\right] + \frac{1}{2}\sum_{k=1}^{K}\mathbb{E}\left[R_k^2(t)\right] + \frac{1}{2}\mathbb{E}\left[P_{ave}^2(t)\right] \\
&\quad + \frac{1}{2}\mathbb{E}\left[Y^2(t)\right] + \frac{1}{2}\sum_{k=1}^{K}\mathbb{E}\left[Q_k^2(t)\right] \\
&\quad + \frac{1}{2}\sum_{k=1}^{K}\mathbb{E}\left[C_k^2(t)D_k^2(t)\right]
\end{aligned} \tag{16}$$

And there is an upper bound B for $B(t)$. It is easy to find that

$$\begin{aligned}
&\Delta[\mathbf{G}(\mathbf{t})] - V\mathbb{E}\left[\sum_{k=1}^{K} U_k(t) \mid \mathbf{G}(\mathbf{t})\right] \\
&\le B + \sum_{k=1}^{K} Q_k(t)\,\mathbb{E}\left[R_k(t) - C_k(t) \mid \mathbf{G}(\mathbf{t})\right] \\
&\quad + E(t)\,\mathbb{E}\left[Y(t) - P_{ave} \mid \mathbf{G}(\mathbf{t})\right] \\
&\quad + \sum_{k=1}^{K} Z_k(t)\,\mathbb{E}\left[Q_k(t) - C_k(t)D_k(t) \mid \mathbf{G}(\mathbf{t})\right] \\
&\quad - V\mathbb{E}\left[\sum_{k=1}^{K} U_k(t) \mid \mathbf{G}(\mathbf{t})\right]
\end{aligned} \tag{17}$$

According to the design principle of Lyapunov optimization, (9) is rearranged as

$$\begin{aligned}\min_{\mathbf{R(t),P(t),w(t)}} \quad & \sum_{k=1}^{K} Q_k(t)\left[R_k(t) - C_k(t)\right] + E(t)\left[\sum_{k=1}^{K} P_k(t) - P_{ave}\right] \\ & + \sum_{k=1}^{K} Z_k(t)\left[Q_k(t) - C_k(t)D_k(t)\right] - V\left[\sum_{k=1}^{K} U_k(t)\right] \quad (18)\\ s.t. \quad & C2, C5, C6, C7, C8 \\ \text{Queue} \quad & Q_k(t), Z_k(t), \forall k, \text{and } E(t) \text{ are mean rate stable.}\end{aligned}$$

5.2. Online Algorithm Design. Shown as (18), the long-term optimization (9) is transferred to a series of single slot optimization problems. Further, (18) could be decomposed into two subproblems, due to none coupling constraints at single slot. One is the RC subproblem in the network layer. The other one is the RSPA subproblem in the physical layer.

The RC subproblem is illustrated as

$$\begin{aligned}&\text{RC}\\ \min_{\mathbf{R(t)}} \quad & \sum_{k=1}^{K}\left[Q_k(t)R_k(t) - VU_k(t)\right] \quad (19)\\ s.t. \quad & C8\end{aligned}$$

Because $U_k(t)$ is a concave function of $R_k(t)$. The RC subproblem is a convex optimization problem. This problem is easy to be solved using the Lagrangian multiplier method. Observing the objective of RC subproblem, it is found that RC results are affected by factors such as $Q_k(t)$, V, and χ_k.

In addition, the RSPA subproblem is shown as

$$\begin{aligned}\min_{\mathbf{P(t),w(t)}} \quad & \sum_{k=1}^{K} Z_k(t)\left[Q_k(t) - C_k(t)D_k(t)\right] \\ & - \sum_{k=1}^{K}\left[Q_k(t)C_k(t)\right] \quad (20)\\ & + E(t)\left[\sum_{k=1}^{K} P_k(t) - P_{ave}\right] \\ s.t. \quad & C2, C5, C6, C7\end{aligned}$$

Consider that the definition of $Z_k(t)$ indicates the demand to transmit traffic data in time; otherwise, the traffic data will be backlogged, note that $Q_k(t) - C_k(t)D_k(t)$ should be limited by $\max[Q_k(t) - C_k(t)D_k(t), 0]$. So (20) can be regulated as

$$\begin{aligned}&\text{RSPA}\\ \min \quad & J \\ & = \sum_{k=1}^{K} Z_k(t)\max\left[Q_k(t) - C_k(t)D_k(t), 0\right] \\ & - \sum_{k=1}^{K}\left[Q_k(t)C_k(t)\right] \\ & + E(t)\left[\sum_{k=1}^{K} P_k(t) - P_{ave}\right] \\ s.t. \quad & C2, C5, C6, C7\end{aligned} \quad (21)$$

Lemma 1. *$\partial J/\partial P_k(t)$ is a function that is only limited by $P_k(t)$. The second-order partial derivative $\partial^2 J/\partial P_k(t)\partial P_i(t)$ is 0 (when $k \neq i$) or positive real value (when $k = i$).*

Lemma 2. *The Hessian matrix of J for $\mathbf{P(t)} = [P_1(t), P_2(t), \cdots P_K(t)]$ is a diagonal matrix and its eigenvalues are all positive.*

Lemmas 1 and 2 are proved in Appendix A.

Theorem 3. *Given the relay selection results, the Hessian matrix of J for $\mathbf{P(t)} = [P_1(t), P_2(t), \cdots P_K(t)]$ is a positive definite matrix, and RSPA is a convex function for $\mathbf{P(t)} = [P_1(t), P_2(t), \cdots P_K(t)]$.*

Proof. Theorem 3 is proved with Lemmas 1 and 2. Further, it is inferred that RSPA is a convex optimization problem, when the mobile relay selection results are given. □

5.3. Matching-Based Mobile Relay Selection. RSPA is a mixed integer nonlinear programming problem. And its constraints $C6$ and $C7$ guarantee that there is one-to-one correspondence among queues and mobile relays. Theorem 3 proves that, given the mobile relay selection results, the power allocation problem is a convex problem. Thus the price-based matching algorithm is proposed to get the mobile relay selection results [30].

The matching problem can be described as a triple $[\mathbf{K}, \mathbf{N}, \mathcal{F}(t)]$. Queue $\mathbf{K}$ for different users is one of the matching participants. The other one participant is mobile relays $\mathbf{N}$. $\mathcal{F}(t)$ is the matching preference matrix.

Matching at timeslot t is defined by the following: For the mobile relay selection problem $[\mathbf{K}, \mathbf{N}, \mathcal{F}(t)]$ based on matching, the matching Ψ is a one-to-one correspondence from set $\mathbf{K} \cup \mathbf{N}$ onto itself under preference matrix $\mathcal{F}(t)$; i.e., $\Psi(\mathbf{K}) \in \mathbf{N}, \forall k \in \mathbf{K}$. $\Psi(k) = n$ represents that queue k is matched with the mobile relay n, that equals $w_{k,n}(t) = 1$.

In order to minimize the RSPA problem, we can define that the preference as

$$\begin{aligned}\mathbb{F}_{k,n}\big|_{\Psi(k)=n} = {} & Q_k(t)C_k(t) - E(t)P_k(t) \\ & - Z_k(t)\max\left[Q_k(t) - C_k(t)D_k(t), 0\right] \quad (22)\\ & - \Theta_n(t)\end{aligned}$$

where $\Theta_n(t)$ is the price for selecting the mobile relay n, which is used to resolve the conflict of the matching process.

Obtaining the preference matrix $\mathcal{F}(t)$: First, queue of user k is paired with every channel. Second, obtain $\mathcal{F}_k(t)$

(1) **Initialization:**
Calculate $\mathcal{F}_k(t)$ for each queue.
Initialize Ψ as an empty set. The set of mobile relays which receive more than one matching proposal from queues is defined as $\Omega(t)$, $\Omega(t) = \varnothing$ at the beginning.
For any mobile relay $n \in N$, setting $\Theta_n(t) = 0$
(2) **Repeating:**
If $\exists\Psi(k) = \varnothing$, preform the rule of matching k with the mobile relay who has the maximum preference according to Equation (22).
Each queue $k \in K$ proposes to its most preferred vehicle in its preference list $\mathcal{F}_k(t)$.
If any mobile relay $n \in N$ receives only one proposal from a queue, then n will be directly matched with the mobile relay which sends the initial proposal. Otherwise, add n in to set $\Omega(t)$.
If $\Omega(t) \neq \varnothing$, perform the price rising rule for mobile relays which received more than one matching proposal.
Each mobile relay $n \in \Omega(t)$ increase its price by adding $\Delta\Theta_n$.
Every queue which has proposed to n updates its preference towards n and remews its proposal.
Remove the vehicles which receive only proposal from $\Omega(t)$.
End Every queue has been matched with a mobile relay.

Algorithm 1: Price-Based Matching Algorithm.

(1) **Input:** K, N, T, V, P_{ave}
(2) **Output:** $\mathbf{R}^*(\mathbf{t})$, $\mathbf{P}^*(\mathbf{t})$, $\mathbf{w}^*(\mathbf{t})$
(3) **Initialization:** $t = 0, Q_k(0) = 1, Z_k(0) = 0, E(0) = 0, T = 200$
(4) **While** $t < T$ do
(5) **RC:**
(6) Obtain the optimal solution $\mathbf{R}^*(\mathbf{t})$ by solving RC
(7) **RSPA:**
(8) Update the channel state due to the mobility of vehicles
(9) Use **matching** to generate the result of mobile relay selection $\mathbf{w}^*(\mathbf{t})$
(10) Given $\mathbf{w}^*(\mathbf{t})$, obtain the optimal solutions set $\mathbf{P}^*(\mathbf{t})$
(11) **Update the queue by**
$Q_k(t+1) = \max[Q_k(t) - C_k(t), 0] + R_k^*(t)$,
$E(t+1) = \max[E(t) - P_{ave}, 0] + Y^*(t)$,
$Z_k(t+1) = \max[Z_k(t) - C_k(t)D_k(t), 0] + Q_k(t)$
(12) $t = t + 1$
(13) **end while**

Algorithm 2: Online Algorithm Based on Lyapunov Optimization.

by selecting the maximum value using (22). Third, $\mathcal{F}(t)$ is obtained by repeating the first and second steps.

Then the price-based matching algorithm is introduced as Algorithm 1.

The comprehensive theoretical analyses of matching on convergence, stability, optimality, and complexity have been proved in [31]. According to the three facts: (1) RC being a convex problem; (2) matching which could complete the mobile relay selection problem; (3) Theorem 3, (9) could be solved by Algorithm 2.

In Algorithm 2, $\mathbf{R}^*(\mathbf{t})$ and $\mathbf{P}^*(\mathbf{t})$ are the optimal RC and power allocation solutions at timeslot t. $Y^*(t)$ is the sum of the energy consumption of BS.

5.4. Performance Analysis. The aim of this work is to solve the long-term optimization (9). With the assist of Lyapunov optimization approach, this problem is converted into the online single timeslot optimization problem. If the single timeslot optimization is solved optimally at each timeslot, the optimal solution to the original problem can then be achieved asymptotically, following an $[O(V), O(1/V)]$ trade-off between the queue backlogs and the achieved utility, which is given in Theorem 4.

Theorem 4. *Bounds of the optimal utility and the average congestion satisfy*

$$\lim_{T\longrightarrow\infty}\frac{1}{T}\sum_{t=1}^{T}\mathbb{E}\left[\sum_{k=1}^{K}U_k(t)\right] \geq U^* - \frac{B}{V}$$
$$\lim_{T\longrightarrow\infty}\frac{1}{T}\sum_{t=1}^{T}\mathbb{E}\left[\sum_{k=1}^{K}Q_k(t)\right] \leq \frac{B + V\left(U_{\max} - U^*\right)}{\varepsilon} \tag{23}$$

Theorem 4 has been proved in Appendix B. $O(V)$ shows the size of queue backlog. $O(1/V)$ shows the gap between the acquired utility and the possible maximum value. When V is large

enough, the utility could be considered as the maximum utility, with the worst queue backlog.

Actually, Algorithm 2 based on the V2X communication system is easy to be operated in practice, with low complexity. We can assume that a large number of users walking in the commercial street produce massive traffic demands. However, the restricted power could not support all users' requirements, reducing the QoE. Then the vehicles with communication modules on the roadside can give the help.

Algorithm 2 will be started for the service request from K users to BS. At the first step, there are downlink traffic arrivals, and then the BS network layer starts the traffic control function. The RC subproblem will be solved by standard convex optimization effectively.

At the second step, BS will select the optimal mobile relay according to the current channel information which could be obtained through the help of mobile relays. In the process of price-based matching, the complexity for each queue to acquire the preferences of all the vehicles and the complexity for sorting the obtained preferences are $O(N)$ and $O(N)\log(N)$. Assume that the conflicting elements are matched within ξ iterations. The mobile relay selection is solved with matching whose complexity is $O(\xi N)\log(N)$.

At the third step, under the mobile relay selection results, BS will allocate the limited power to users according to RSPA. Theorem 3 tells that the power allocation is a convex optimization, so the power allocation is also able to be solved with standard convex optimization. Last, BS will update the current information via (1), (10), and (11) for the next timeslot. And the traffic will be transmitted to users by the multihop links.

Moreover, we can find the system will be stabilized after several timeslots, which will be illustrated in the simulation results. And the V2X communication system could support higher performance to users.

6. Simulation Results and Discussions

In this section, simulation results are presented. The stability and tradeoff between utility and queue backlog are analyzed. What is more, we compare long-term performance of two communication system, including the V2X multihop communication system in this paper and the traditional direct link communication system. For convenience, the work of long-term optimization with AF (LTAF) under V2X multihop communication system is called LTAF, and similarly the work of long-term optimization with direct link (LTDL) is called LTDL. The simulation parameters have been illustrated in Table 1.

6.1. Stability. As expected, the queues $Q_k(t)$, $Z_k(t)$, and $E(t)$ tend to stabilize over time, which are shown in Figures 3, 4, and 5. As a result, the system's utility finally remains stable so as the arrival rate and transmission capacity do, which are shown in Figures 6, 7, and 8. Moreover, Figure 9(a) reflects changes of actual delay. Figure 9(b) tells the fact that the average actual delay is lower than the demand, and its variance is small in the allowable range.

Table 1: Simulation parameters.

Parameters	Value
$\mathbf{Q}(\mathbf{0})$	[1, 1, 1, 1] Mbits
$\mathbf{D}(\mathbf{t})$	[250, 500, 800, 1000]ms
$\mathbf{Z}(\mathbf{0})$	[0, 0, 0, 0]
$E(0)$	0 watts
$P_{\max}$	2.5 watts
P_{ave}	8 watts
$R_{\max}$	50 Mbps
$K = N$	4
$\Delta\Theta_n$	0.1

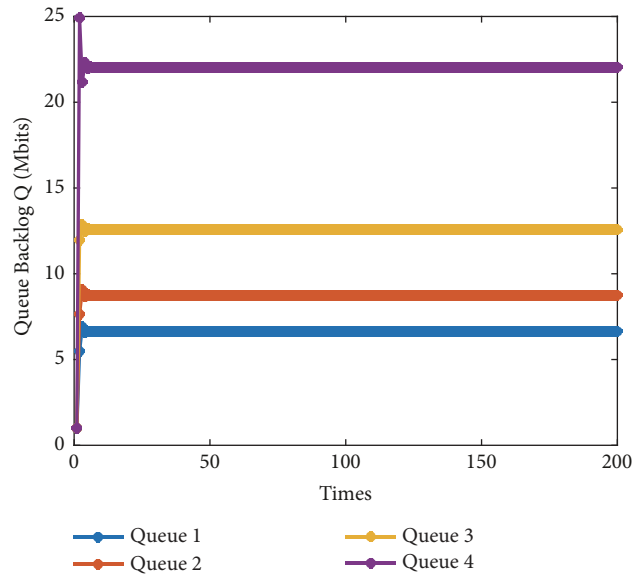

Figure 3: Queue backlogs versus time.

At the same time, the stability of queues reveals three issues:

(i) The robustness of queue congestion is guaranteed. In other words, the queue backlog is limited in a controllable range. So the system will not crash due to heavy traffic owing to the rate control of BS.

(ii) The latency requirements of users are satisfied. Moreover, the actual delay is always lower than the upper bound of delay, shown as Figure 9.

(iii) The limited power resource is used effectively, and the long-term power constraint is accomplished. If we assume P_{ave} as the energy income at each timeslot, $Y(t)$ as an expenditure at timeslot t, the fluctuations could be explained by the following: if the income exceeds the expenditure, it will be stored for the next timeslot; otherwise, it will borrow energy from other timeslots with the result of generating debt accumulation. Actually, $E(t)$ represents the debt accumulation of power consumption. After long-term observation, it can be found that $E(t)$ fluctuates around a fixed value P_{ave}, and the mean power consumption almost

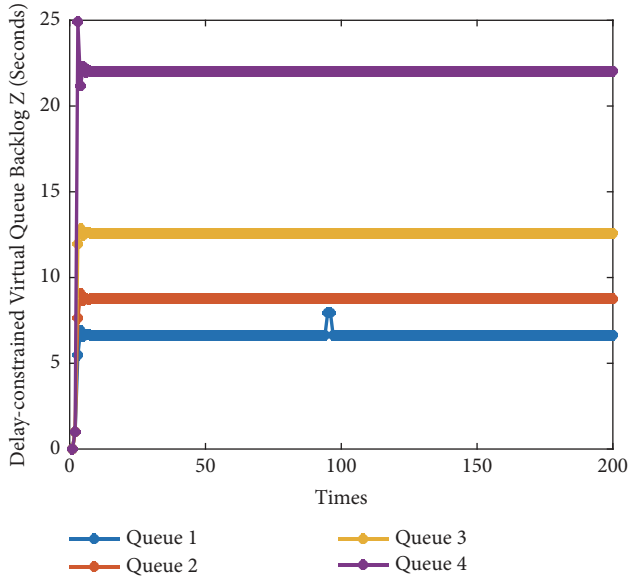

FIGURE 4: Delay-constrained virtual queues versus time.

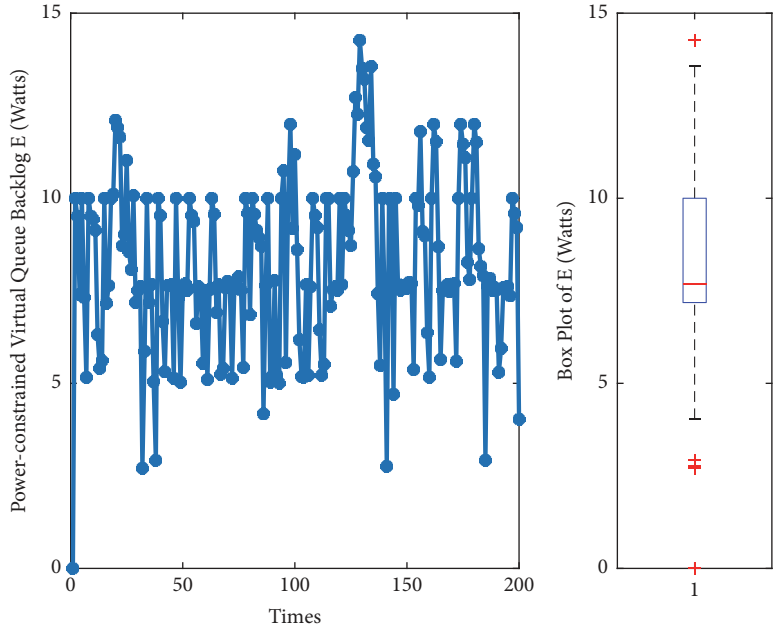

FIGURE 5: Power-constrained virtual queue versus time and the box plot of E.

equals P_{ave} which can be proved by the box plot of Figure 5.

We can find that $Q_k(t)$ and $Z_k(t)$ will equal $R_k(t)$ finally, as time goes. According to Lyapunov optimization, when $Q_k(t)$ is stable, $C_k(t) \geq R_k(t)$ is established. That means traffic will be entirely delivered to users at each timeslot. So, $R_k(t)$ is recorded as the queue backlog for $Q_k(t+1)$, according to (1). Similarly, for $Z_k(t)$, when the system stabilizes, $Q_k(t)$ is recorded as the queue backlog for $Z_k(t+1)$.

In addition, we can find $C_k(t)$ is far higher than $R_k(t)$, for Queue 1, Queue 2, and Queue 3. That could be deduced by the stability conditions of delay-constrained virtual queue. The stability of $Z_k(t)$ requires $C_k(t)D_k(t) \geq Q_k(t)$, where $D_k(t)$ is a constant less than 1 second.

6.2. Tradeoff. Firstly, we will explain the baseline. Baseline is the results of individually optimizing the utility and transmission capacity, respectively. LTAF is the result of our algorithm. Figure 10 is the plots of utility versus $V$and queue backlog versus V.

For LTAF, we can observe that the utility is in inverse proportion to V, and the queue backlog is proportional to V. These results respond to Theorem 4. More importantly,

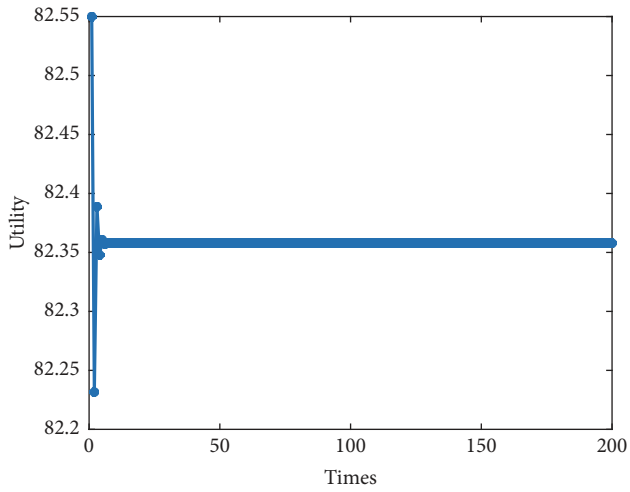

Figure 6: Utility versus time.

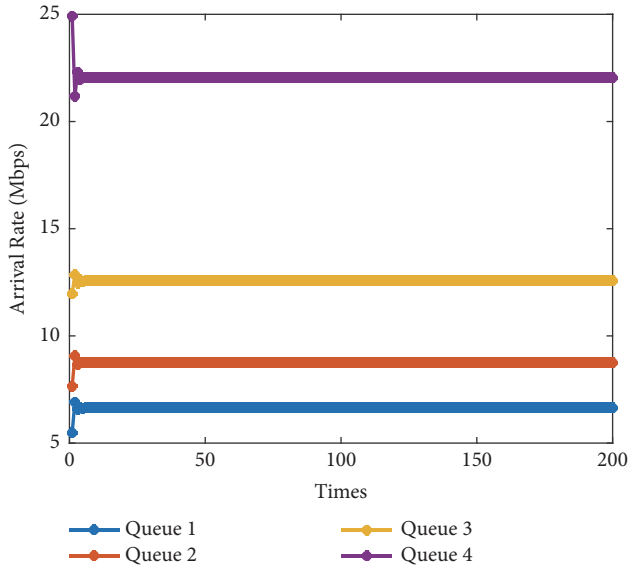

Figure 7: Arrival rate versus time.

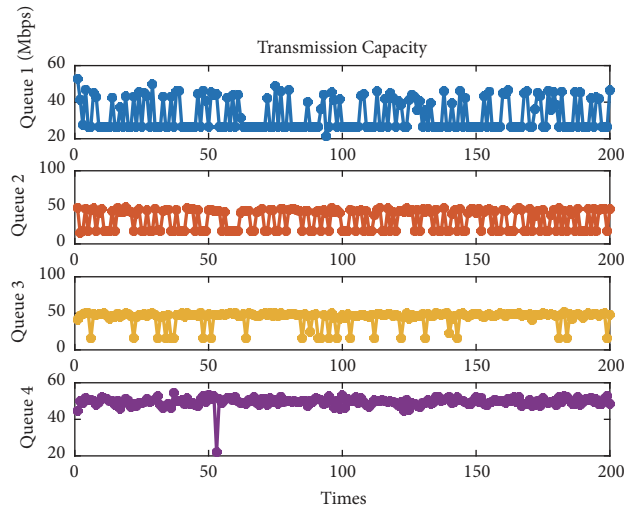

Figure 8: Transmission capacities versus time.

the utility gap between LTAF and baseline decreases, as V becomes larger. In fact, baseline stands for the optimal value of utility and queue backlog. Further, Figure 10 shows that the results acquired by LTAF is infinitely close to the optimal utility, with the increase of V. However, the queue backlog is almost equal to 50 Mbps, the worst queue backlog. These phenomena highlight tradeoff relationship between utility and queue backlog.

6.3. Comparison. In this part, the main work is to compare the performance of queue backlog Q, delay-constrained virtual queue Z, and power-constrained virtual queue E of LTAF and LTDL.

Figure 11 illustrates the queue backlog Q of LTDL and error bar comparisons of LTAF and LTDL on Q. Comparing Figure 11 with Figure 3, though Q of LTDL finally becomes stable, bad points often occur. These bad points bring the larger fluctuation to LTDL, so its variance is larger than LTAF, which is shown in Figure 11.

In Figure 12, there are the plot of delay-constrained virtual queue Z versus time for LTDL and error bar comparisons of LTAF and LTDL on Z. In Figure 12, the delay-constrained virtual queue backlog of Queue 1 is unstable. That means the delay constraint for user 1 could not be met. The delay requirements of the other three queues are satisfied, but there are also many bad points. As a result, variance on Z of LTDL is larger than LTAF.

In Figures 11 and 12, these bad points and exceeded allowable fluctuations present the possibility that users' instant constraints are not guaranteed. That means LTDL communication system possesses worse instantaneous performance.

Figure 13 is the plot of power-constrained virtual queue E versus time for LTDL and error bar comparisons of LTAF and LTDL on E. Comparing with Figure 5, the queue E of LTDL climbs quickly firstly and then began to increase gently. That indicates that BS always consumes the available maximum power at each timeslot. Conversely, the power consumption of BS under LTAF is enough due to the assist of vehicles. From the perspective of power consumption, LTDL brings more pressure on the operators to maintain BSs. Because BSs are more susceptible to damage for working at the maximum power.

7. Conclusions

In this paper, a cross-layer resource allocation schemes for V2X communication system was investigated. First, the downlink transmission for BS with the help of vehicles as mobile relays was proposed. These mobile relays play roles in extending the coverage distance of the BS and increasing the capacity. Second, to establish the cross-layer resource allocation problem, the queue model was applied to couple the arrival rate in the network layer with the transmission capacity in the physical layer. Third, Lyapunov optimization was proposed to transfer the long-term optimization problem to series of rate control and mobile relay selection-power allocation problems at each timeslot. And the tradeoff between queue backlog and utility was evaluated. Fourth, expecting

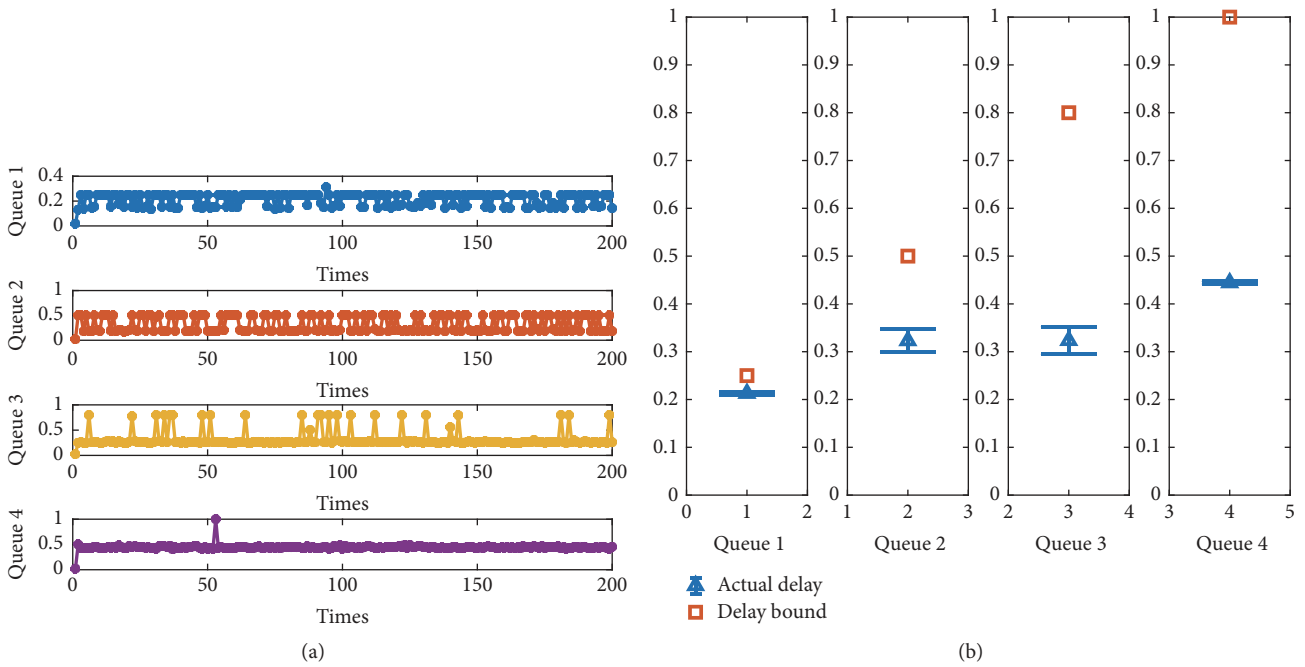

FIGURE 9: Actual delay. (a) Actual delay versus time. (b) The bound and average actual delay of different queues. The error bars represent the variance of measurements for 200 timeslots.

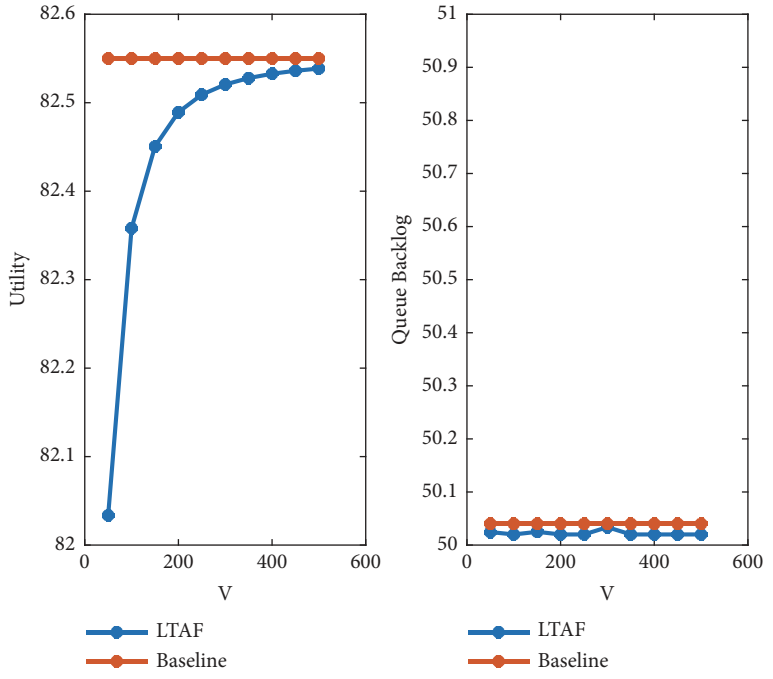

FIGURE 10: The tradeoff between utility and queue backlog versus V.

low computational complexity, the mobile relay selection was optimized with matching. Then simulation results verified that LTAF could reach the stability as expected; LTAF could obtain the optimal utility with the worst queue backlog; and LTAF not only could reduce the burden on BSs but also could satisfy the diversity requirements of user business; i.e., LTAF could accomplish the latency demands of different queues at each time slot but the LTDL could not.

In future work, we will focus on rental-based relay selection problem for V2X communication system. In this paper, the vehicle is a free boost for BS. In fact, the vehicle, as a private property, is difficult to open for users freely.

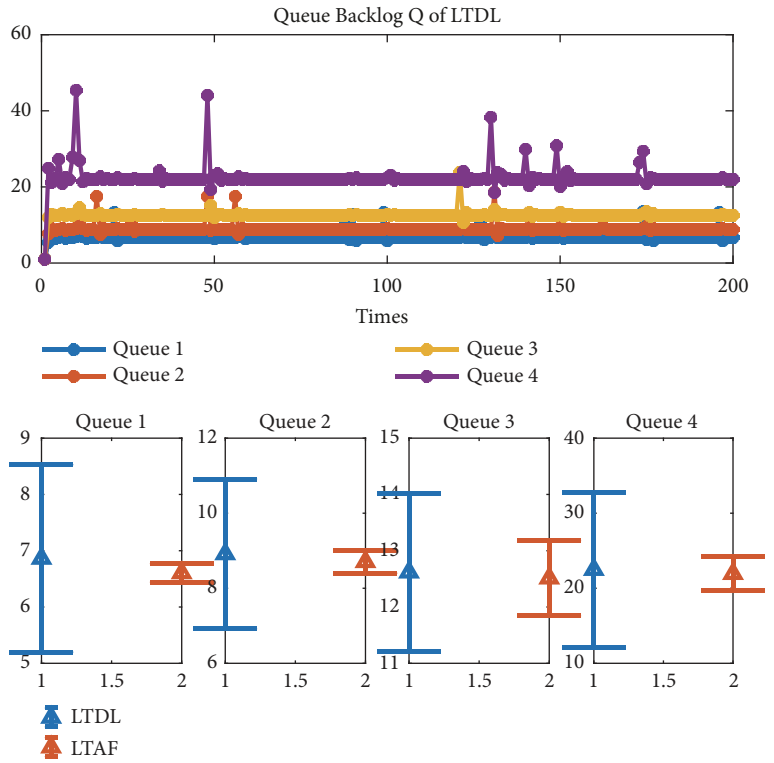

FIGURE 11: Queue backlog of LTDL versus time and error bar for comparison. The error bars represent the variance of measurements for 200 timeslots.

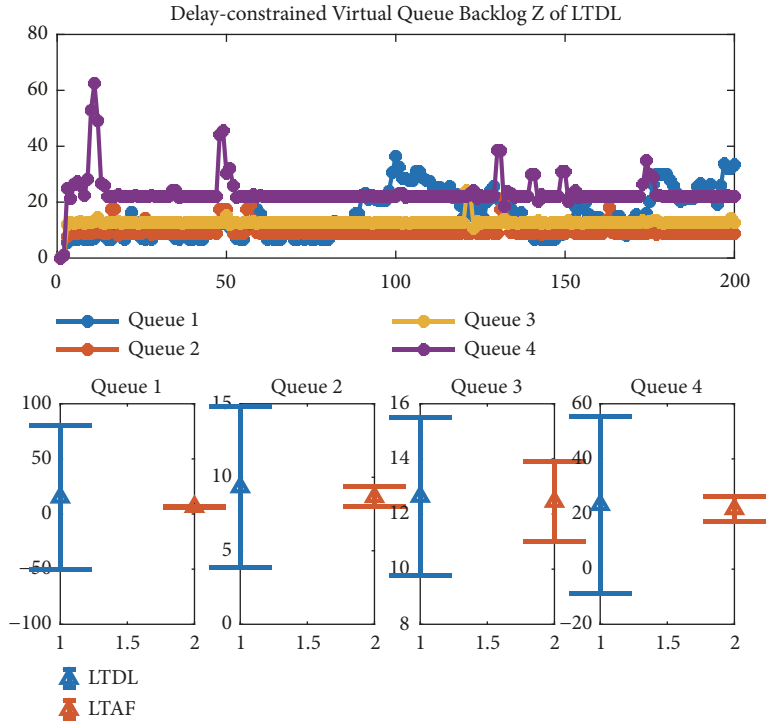

FIGURE 12: Delay-constrained virtual queue backlog of LTDL versus time and error bar for comparison. The error bars represent the variance of measurements for 200 timeslots.

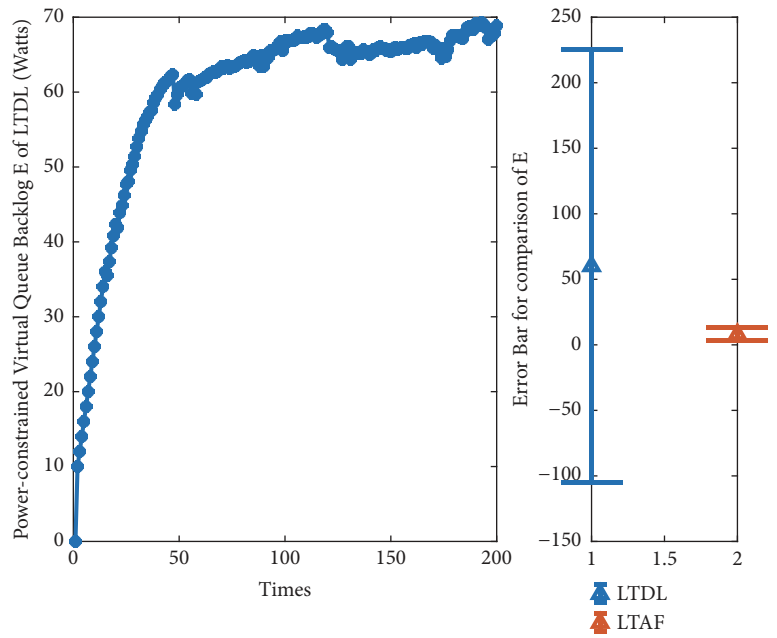

FIGURE 13: Power-constrained virtual queue backlog of LTDL versus time and error bar for comparison. The error bars represent the variance of measurements for 200 timeslots.

Appendix

A. Proof of Lemmas 1 and 2

To prove Lemma 1, the first-order partial derivative $\partial J/\partial P_k(t)$ of J with regard to $P_k(t)$ is calculated:

$$\frac{\partial J}{\partial P_k(t)} = \begin{cases} -Q_k(t)\dfrac{\partial C_k(t)}{\partial P_k(t)} + E_k(t) & Q_k(t) \le C_k(t) D_k(t) \\ -Q_k(t)\dfrac{\partial C_k(t)}{\partial P_k(t)} - Z_k(t) D_k(t)\dfrac{\partial C_k(t)}{\partial P_k(t)} + E_k(t) & \text{otherwise} \end{cases} \tag{A.1}$$

where $\partial C_k(t)/\partial P_k(t) = (F/2\ln(2))((b_k(t)c_k(t) + b_k(t)c_k^2(t))/((1 + a_k(t)P_k(t))(1 + b_k(t)P_k(t) + c_k(t)) + b_k(t)P_k(t)c_k(t))(1 + b_k(t)P_k(t) + c_k(t)))$ and $a_k(t) = |h_{k,u}(t)|^2/\sigma^2 > 0$, $b_k(t) = |h_{k,n}(t)|^2/\sigma^2 > 0$, $c_k(t) = P_r(t)|h_{n,u}(t)|^2/\sigma^2 > 0$.

Then, the second-order partial derivative $\partial^2 J/\partial P_k(t)\partial P_i(t)$ is calculated:

$$\begin{aligned} &\frac{\partial^2 J}{\partial P_k(t)\,\partial P_i(t)} = 0 \quad k \ne i \\ &\frac{\partial^2 J}{\partial P_k^2(t)} = \frac{FQ_k(t)\left[b_k(t)c_k(t) + b_k(t)c_k^2(t)\right]\left[\partial g_k(t)/\partial P_k(t)\right]}{2\ln(2)\, g_k^2(t)} > 0 \quad \text{when } Q_k(t) \le C_k(t) D_k(t) \\ &\frac{\partial^2 J}{\partial P_k^2(t)} = \frac{F\left[Q_k(t) + Z_k(t) D_k(t)\right]\left[b_k(t)c_k(t) + b_k(t)c_k^2(t)\right]\left[\partial g_k(t)/\partial P_k(t)\right]}{2\ln(2)\, g_k^2(t)} > 0 \\ &\qquad\qquad \text{when } Q_k(t) > C_k(t) D_k(t) \end{aligned} \tag{A.2}$$

Here, $g_k(t) = \{[1 + a_k(t)P_k(t)][1 + b_k(t)P_k(t) + c_k(t)] + b_k(t)P_k(t)c_k(t)\}[1 + b_k(t)P_k(t) + c_k(t)]$, and $\partial g_k(t)/\partial P_k(t) > 0\ \forall k$.

Combining the results of (A.1) and (A.2), Lemmas 1 and 2 are proven.

B. Proof of Theorem 4

At first, we assume that, under such V2X multihop communication system, the expectation of $U(t)$ satisfies

$$U_{\min} \le U(t) \le U_{\max} \tag{B.1}$$

Here, $U(t) = \sum_{k=1}^{K} U_k(t)$. The assumption is feasible, because of the limitations for physical channel, transmission rate, and power consumption.

After a certain number of iterations as Algorithm 2, the system will tend to stabilize. Then, there are three arbitrarily small positive numbers ε_1, ε_2, and ε_3; those satisfy

$$\begin{aligned}\mathbb{E}\left[R_k(t) - C_k(t) \mid \mathbf{G}(\mathbf{t})\right] &= \mathbb{E}\left[\widetilde{R_k}(t) - \widetilde{C_k}(t)\right] \le -\varepsilon_1 \\ &\le -\varepsilon\end{aligned} \tag{B.2}$$

$$\mathbb{E}\left[Y(t) - P_{ave} \mid \mathbf{G}(\mathbf{t})\right] = \mathbb{E}\left[\widetilde{Y}(t) - P_{ave}\right] \le -\varepsilon_2 \le -\varepsilon \tag{B.3}$$

$$\begin{aligned}&\mathbb{E}\left[Q_k(t) - C_k(t) D_k(t) \mid \mathbf{G}(\mathbf{t})\right] \\ &\quad = \mathbb{E}\left[\widetilde{Q_k}(t) - \widetilde{C_k}(t)\,\widetilde{D_k}(t)\right] \le -\varepsilon_3 \le -\varepsilon\end{aligned} \tag{B.4}$$

$$\mathbb{E}\left[U(t) \mid \mathbf{G}(\mathbf{t})\right] = \mathbb{E}\left[\widetilde{U}(t)\right] = U^* \tag{B.5}$$

$$\varepsilon = \min\left(\varepsilon_1, \varepsilon_2, \varepsilon_3\right) \tag{B.6}$$

where $\widetilde{R_k}(t)$, $\widetilde{C_k}(t)$, $\widetilde{Y}(t)$, $\widetilde{D_k}(t)$, and $\widetilde{U}(t)$ are the resulting admission rate, the transmission capacity, power consumption, and QoE under any alternative decision; U^* is the theoretical optimum of (9) [32].

This paper focuses on minimizing the drift-minus-function. Plugging (B.2), (B.3), and (B.4) to (17), we could have

$$\begin{aligned}&\Delta\left[\mathbf{G}(\mathbf{t})\right] - V\mathbb{E}\left[\sum_{k=1}^{K} U_k(t) \mid \mathbf{G}(\mathbf{t})\right] \\ &\quad \le B - V\mathbb{E}\left[U^* \mid \mathbf{G}(\mathbf{t})\right] - \varepsilon\left[\sum_{k=1}^{K} Q_k(t)\right]\end{aligned} \tag{B.7}$$

By taking the iterated expectation and using telescoping sums over $t \in \{0, 1, 2, \cdots, T-1\}$, (B.8) can be derived:

$$\begin{aligned}&\mathbb{E}\left\{L\left[\mathbf{G}(\mathbf{t}+\mathbf{1})\right]\right\} - \mathbb{E}\left\{L\left[\mathbf{G}(0)\right]\right\} \\ &\quad - V\mathbb{E}\left[\sum_{t=0}^{T-1}\sum_{k=1}^{K} U_k(t)\right] \\ &\quad \le TB - VTU^* - \varepsilon\left[\sum_{t=0}^{T-1}\sum_{k=1}^{K} Q_k(t)\right]\end{aligned} \tag{B.8}$$

Then, rearranging (B.8), we can have

$$\begin{aligned}&\mathbb{E}\left\{L\left[\mathbf{G}(\mathbf{t}+\mathbf{1})\right]\right\} - \mathbb{E}\left\{L\left[\mathbf{G}(0)\right]\right\} \\ &\quad \le TB - VTU^* - \varepsilon\left[\sum_{t=0}^{T-1}\sum_{k=1}^{K} Q_k(t)\right] \\ &\qquad + V\mathbb{E}\left[\sum_{t=0}^{T-1}\sum_{k=1}^{K} U_k(t)\right] \\ &\quad \le TB - VTU^* - \varepsilon\left[\sum_{t=0}^{T-1}\sum_{k=1}^{K} Q_k(t)\right] + VTU_{\max}\end{aligned} \tag{B.9}$$

Both sides of the above inequality are divided by εT. Then we can obtain

$$\begin{aligned}&\frac{1}{T}\left[\sum_{t=0}^{T-1}\sum_{k=1}^{K} Q_k(t)\right] \\ &\quad \le \frac{B + V\left(U_{\max} - U^*\right)}{\varepsilon} \\ &\qquad + \frac{\mathbb{E}\left\{L\left[\mathbf{G}(0)\right]\right\} - \mathbb{E}\left\{L\left[\mathbf{G}(\mathbf{t}+\mathbf{1})\right]\right\}}{T}\end{aligned} \tag{B.10}$$

Note $\lim_{T\to\infty}(\mathbb{E}\{L[\mathbf{G}(0)]\} - \mathbb{E}\{L[\mathbf{G}(\mathbf{t}+\mathbf{1})]\}/T) = 0$. Equation (B.11) is deduced as

$$\lim_{T\to\infty} \frac{1}{T}\sum_{t=0}^{T-1}\sum_{k=1}^{K} Q_k(t) \le \frac{B + V\left(U_{\max} - U^*\right)}{\varepsilon} \tag{B.11}$$

Similarly, (B.15) can be derived by shifting shown as (B.12), relaxing shown as (B.13), and calculating limits shown as (B.14).

$$\begin{aligned}&V\mathbb{E}\left[\sum_{t=0}^{T-1}\sum_{k=1}^{K} U_k(t)\right] \\ &\quad \ge \mathbb{E}\left\{L\left[\mathbf{G}(\mathbf{t}+\mathbf{1})\right]\right\} - \mathbb{E}\left\{L\left[\mathbf{G}(0)\right]\right\} - TB \\ &\qquad + VTU^* + \varepsilon\left[\sum_{t=0}^{T-1}\sum_{k=1}^{K} Q_k(t)\right]\end{aligned} \tag{B.12}$$

$$\begin{aligned}&V\mathbb{E}\left[\sum_{t=0}^{T-1}\sum_{k=1}^{K} U_k(t)\right] \\ &\quad \ge \mathbb{E}\left\{L\left[\mathbf{G}(\mathbf{t}+\mathbf{1})\right]\right\} - \mathbb{E}\left\{L\left[\mathbf{G}(0)\right]\right\} - TB \\ &\qquad + VTU^*\end{aligned} \tag{B.13}$$

$$\begin{aligned}&\frac{1}{T}\mathbb{E}\left[\sum_{t=0}^{T-1}\sum_{k=1}^{K} U_k(t)\right] \\ &\quad \ge \frac{\mathbb{E}\left\{L\left[\mathbf{G}(\mathbf{t}+\mathbf{1})\right]\right\} - \mathbb{E}\left\{L\left[\mathbf{G}(0)\right]\right\}}{VT} - \frac{B}{V} + U^*\end{aligned} \tag{B.14}$$

$$\lim_{T\to\infty} \frac{1}{T}\mathbb{E}\left[\sum_{t=0}^{T-1}\sum_{k=1}^{K} U_k(t)\right] \ge U^* - \frac{B}{V} \tag{B.15}$$

Data Availability

The data used to support the findings of this study are included within the article. The data is shown in Table 1.

Conflicts of Interest

The authors declare that they have no conflicts of interest.

Acknowledgments

Professor Zhenyu Zhou provided help during the research and preparation of the manuscript. And this work is supported by the Fundamental Research Funds for the Central Universities (2018QN003).

References

[1] B. Fekade, T. Maksymyuk, and M. Jo, "Clustering hypervisors to minimize failures in mobile cloud computing," *Wireless Communications and Mobile Computing*, vol. 16, no. 18, pp. 3455–3465, 2016.

[2] Z. Zhang, H. Sun, and R. Q. Hu, "Downlink and uplink non-orthogonal multiple access in a dense wireless network," *IEEE Journal on Selected Areas in Communications*, vol. 35, no. 12, pp. 2771–2784, 2017.

[3] T. Sahin, M. Klugel, C. Zhou, and W. Kellerer, "Virtual cells for 5G V2X communications," *IEEE Communications Standards Magazine*, vol. 2, no. 1, pp. 22–28, 2018.

[4] W. Sun, D. Yuan, E. G. Ström, and F. Brännström, "Cluster-based radio resource management for D2D-supported safety-critical V2X communications," *IEEE Transactions on Wireless Communications*, vol. 15, no. 4, pp. 2756–2769, 2016.

[5] B. Di, L. Song, Y. Li, and G. Y. Li, "Non-orthogonal multiple access for high-reliable and low-latency V2X communications in 5G systems," *IEEE Journal on Selected Areas in Communications*, vol. 35, no. 10, pp. 2383–2397, 2017.

[6] S. Lien, S. Hung, D. Deng, C. Lai, and H. Tsai, "Low latency radio access in 3GPP local area data networks for V2X: Stochastic optimization and learning," *IEEE Internet of Things Journal*, vol. 2, no. 1, 2018.

[7] Z. Zhou, J. Feng, B. Gu et al., "When mobile crowd sensing meets UAV: energy-efficient task assignment and route planning," *IEEE Transactions on Communications*, vol. 66, no. 11, pp. 5526–5538, 2018.

[8] Z. Zhou, H. Yu, C. Xu, Y. Zhang, S. Mumtaz, and J. Rodriguez, "Dependable content distribution in D2D-based cooperative vehicular networks: A big data-integrated coalition game approach," *IEEE Transactions on Intelligent Transportation Systems*, vol. 19, no. 3, pp. 953–964, 2018.

[9] S. Chen, J. Hu, Y. Shi et al., "Vehicle-to-everything (v2x) services supported by LTE-based systems and 5G," *IEEE Communications Standards Magazine*, vol. 1, no. 2, pp. 70–76, 2017.

[10] M. I. Ashraf, C.-F. Liu, M. Bennis, W. Saad, and C. S. Hong, "Dynamic resource allocation for optimized latency and reliability in vehicular networks," *IEEE Access*, 2018.

[11] P. S. Bithas, G. P. Efthymoglou, and A. G. Kanatas, "V2V cooperative relaying communications under interference and outdated CSI," *IEEE Transactions on Vehicular Technology*, vol. 67, no. 4, pp. 3466–3480, 2018.

[12] S. Park, B. Kim, H. Yoon, and S. Choi, "RA-eV2V: Relaying systems for LTE-V2V communications," *Journal of Communications and Networks*, vol. 20, no. 4, pp. 396–405, 2018.

[13] W. Sun, E. G. Strom, F. Brannstrom, Y. Sui, and K. C. Sou, "D2D-based V2V communications with latency and reliability constraints," in *Proceedings of the 2014 IEEE Globecom Workshops (GC Wkshps)*, pp. 1414–1419, Austin, Tex, USA, December 2014.

[14] P. Wang, B. Di, H. Zhang, K. Bian, and L. Song, "Cellular V2X communications in unlicensed spectrum: Harmonious coexistence with VANET in 5G systems," *IEEE Transactions on Wireless Communications*, vol. 17, no. 8, pp. 5212–5224, 2018.

[15] Q. Zheng, K. Zheng, L. Sun, and V. C. M. Leung, "Dynamic performance analysis of uplink transmission in cluster-based heterogeneous vehicular networks," *IEEE Transactions on Vehicular Technology*, vol. 64, no. 12, pp. 5584–5595, 2015.

[16] C.-F. Liu and M. Bennis, "Ultra-reliable and low-latency vehicular transmission: An extreme value theory approach," *IEEE Communications Letters*, vol. 22, no. 6, pp. 1292–1295, 2018.

[17] S. Lakani and F. Gagnon, "Optimal design and energy efficient binary resource allocation of interference-limited cellular relay-aided systems with consideration of queue stability," *IEEE Access*, vol. 5, pp. 8459–8474, 2017.

[18] B. Ravi and J. Thangaraj, "End-to-end delay bound analysis of VANETs based on stochastic method via queueing theory model," in *Proceedings of the 2nd IEEE International Conference on Wireless Communications, Signal Processing and Networking, WiSPNET 2017*, pp. 1920–1923, Chennai, India, March 2017.

[19] J. Mei, K. Zheng, L. Zhao, Y. Teng, and X. Wang, "A latency and reliability guaranteed resource allocation scheme for LTE V2V communication systems," *IEEE Transactions on Wireless Communications*, vol. 17, no. 6, pp. 3850–3860, 2018.

[20] Z. Zhou, F. Xiong, C. Xu, Y. He, and S. Mumtaz, "Energy-efficient vehicular heterogeneous networks for green cities," *IEEE Transactions on Industrial Informatics*, vol. 14, no. 4, pp. 1522–1531, 2018.

[21] Z. Zhou, C. Gao, C. Xu, Y. Zhang, S. Mumtaz, and J. Rodriguez, "Social big-data-based content dissemination in internet of vehicles," *IEEE Transactions on Industrial Informatics*, vol. 14, no. 2, pp. 768–777, 2018.

[22] Y. Ren, F. Liu, Z. Liu, C. Wang, and Y. Ji, "Power control in D2D-based vehicular communication networks," *IEEE Transactions on Vehicular Technology*, vol. 64, no. 12, pp. 5547–5562, 2015.

[23] C. Sacchi, F. Granelli, and C. Schlegel, "A QoE-oriented strategy for OFDMA radio resource allocation based on min-MOS maximization," *IEEE Communications Letters*, vol. 15, no. 5, pp. 494–496, 2011.

[24] J. N. Laneman, D. N. C. Tse, and G. W. Wornell, "Cooperative diversity in wireless networks: efficient protocols and outage behavior," *IEEE Transactions on Information Theory*, vol. 50, no. 12, pp. 3062–3080, 2004.

[25] A. M. K. and M. R. Bhatnagar, "Maximal ratio transmission in af mimo relay systems over nakagami-fading channels," *IEEE Transactions on Vehicular Technology*, vol. 64, no. 5, pp. 1895–1903, 2015.

[26] C.-K. Tseng and S.-H. Wu, "Effective protocols and channel quality control mechanisms for cooperative ARQ with opportunistic AF relaying," *IEEE Transactions on Vehicular Technology*, vol. 67, no. 3, pp. 2382–2397, 2018.

[27] L. Georgiadis, M. J. Neely, and L. Tassiulas, "Resource allocation and cross-layer control in wireless networks," *Foundations and Trends in Networking*, vol. 1, no. 1, pp. 1–144, 2006.

[28] M. J. Neely, "Energy optimal control for time-varying wireless networks," *IEEE Transactions on Information Theory*, vol. 52, no. 7, pp. 2915–2934, 2006.

[29] M. J. Neely, *Stochastic Network Optimization with Application to Communication and Queueing Systems*, Morgan & Claypool Publishers, Calif, USA, 2010.

[30] Z. Zhou, K. Ota, M. Dong, and C. Xu, "Energy-efficient matching for resource allocation in D2D enabled cellular networks," *IEEE Transactions on Vehicular Technology*, vol. 66, no. 6, pp. 5256–5268, 2017.

[31] Y. Gu, W. Saad, M. Bennis, M. Debbah, and Z. Han, "Matching theory for future wireless networks: Fundamentals and applications," *IEEE Communications Magazine*, vol. 53, no. 5, pp. 52–59, 2015.

[32] Y. Guo, Q. Yang, and K. S. Kwak, "Quality-oriented rate control and resource allocation in time-varying OFDMA networks," *IEEE Transactions on Vehicular Technology*, vol. 66, no. 3, pp. 2324–2338, 2017.